

# Surface Morphology Improvement of Non-Polar a-Plane GaN Using a Low-Temperature GaN Insertion Layer \*

Shen Yan(严琄)<sup>1,2</sup>, Xiao-Tao Hu(胡小涛)<sup>1,2</sup>, Jun-Hui Die(迭俊瑋)<sup>1,2</sup>, Cai-Wei Wang(王彩玮)<sup>1,2</sup>, Wei Hu(胡巍)<sup>1,2</sup>, Wen-Liang Wang(王文樑)<sup>3</sup>, Zi-Guang Ma(马紫光)<sup>1,2</sup>, Zhen Deng(邓震)<sup>1,2,4</sup>, Chun-Hua Du(杜春花)<sup>1,2,4</sup>, Lu Wang(王禄)<sup>1,2</sup>, Hai-Qiang Jia(贾海强)<sup>1,2,5</sup>, Wen-Xin Wang(王文新)<sup>1,2,5</sup>, Yang Jiang(江洋)<sup>1,2\*\*</sup>, Guoqiang Li(李国强)<sup>3\*\*</sup>, Hong Chen(陈弘)<sup>1,2,5</sup>

<sup>1</sup>Key Laboratory for Renewable Energy, Beijing Key Laboratory for New Energy Materials and Devices, Beijing National Laboratory for Condensed Matter Physics, Institute of Physics, Chinese Academy of Sciences, Beijing 100190

<sup>2</sup>Center of Materials and Optoelectronics Engineering, University of Chinese Academy of Sciences, Beijing 100049

<sup>3</sup>State Key Laboratory of Luminescent Materials and Devices, South China University of Technology, Guangzhou 510640

<sup>4</sup>The Yangtze River Delta Physics Research Center, Liyang 213000

<sup>5</sup>Songshan Lake Materials Laboratory, Dongguan 523808

(Received 11 November 2019)

We demonstrate that a low-temperature GaN insertion layer could significantly improve the surface morphology of non-polar a-plane GaN. The two key factors in improving the surface morphology of non-polar a-plane GaN are growth temperature and growth time of the GaN insertion layer. The root-mean-square roughness of a-plane GaN is reduced by 75% compared to the sample without the GaN insertion layer. Meanwhile, the GaN insertion layer is also beneficial for improving crystal quality. This work provides a simple and effective method to improve the surface morphology of non-polar a-plane GaN.

PACS: 81.05.Ea, 81.10.St, 81.10.-h

DOI: 10.1088/0256-307X/37/3/038102

Non-polar gallium nitride (GaN) films have attracted a great deal of attention for application in optoelectronic and power electronic devices thanks to the absence of polarized electric field in growth direction.<sup>[1,2]</sup> GaN-based light emitting diodes grown on homoepitaxial non-polar GaN have shown smaller blue shift of luminescence peak and reduced droop effect at high current densities.<sup>[3,4]</sup> Because of its larger size and lower cost, heteroepitaxy is more suitable for industrial production compared to homoepitaxy. Among the heteroepitaxial substrates, sapphire substrates are inexpensive with tolerable lattice mismatch. The lattice mismatch between a-plane GaN and an r-plane sapphire substrate is smaller than that between m-plane GaN and an m-plane sapphire substrate.<sup>[5]</sup> Therefore, growth of a-plane GaN on r-plane sapphire substrates has become a focus of research. Studies of the growth of non-polar a-plane GaN on r-plane sapphire substrates has been carried out since 2002.<sup>[6]</sup> However, the crystal quality of a-plane GaN obtained in the current study still cannot compare with that of c-plane GaN grown on c-plane sapphire substrates.<sup>[7,8]</sup> At present, there are two main problems in heteroepitaxial a-plane GaN: one is the high density of basal plane stacking faults and threading dislocations due to the large lattice and thermal mismatches, and the other is in-plane anisotropy (anisotropy of crystal quality and anisotropy of surface morphology) as a result of the anisotropic adatom diffusion length.<sup>[9]</sup> The anisotropy of surface morphology leads to appearance of surface streaks and an increase

in surface roughness. The emergence of these problems is detrimental to the growth of subsequent device structures. To solve these problems, many different approaches have been proposed, including patterned sapphire substrates with various patterns,<sup>[10–13]</sup> interlayer like SiN<sub>x</sub> and TiN,<sup>[14,15]</sup> and epitaxial lateral overgrowth (ELOG).<sup>[7,16]</sup> These studies mainly focus on improving the crystal quality of a-plane GaN, while there is a lack of research of how to improve the surface morphology of a-plane GaN.

In the present study, we utilize a low-temperature GaN insertion layer to the epitaxial growth of non-polar a-plane GaN films on r-plane sapphire substrates by metal organic chemical vapor deposition (MOCVD). The influence of growth temperature and growth time of the GaN insertion layer on the surface morphology and crystal quality is systematically studied. Introduction of the GaN insertion layer significantly improves the surface morphology of a-plane GaN films, which is helpful to improve the crystal quality. The mechanisms behind the improvement of surface morphology are explored.

The a-plane GaN samples were grown on a 2-inch r-plane sapphire substrate in an Aixtron 2400G3HT LP-MOCVD system. Precursors for gallium, aluminum and nitrogen were trimethylgallium (TMGa), trimethylaluminum (TMAI) and ammonia (NH<sub>3</sub>), respectively. Figure 1 shows the structure of the samples. After annealing under H<sub>2</sub> atmosphere, a 3-nm-thick AlN layer was grown at 880°C. Then, the reactor temperature was increased to 1100°C for a two-

\*Supported by the National Natural Science Foundation of China (Grant Nos. 11574362 and 61704008).

\*\*Corresponding author. Email: jiangyang@iphy.ac.cn; msgli@scut.edu.cn

© 2020 Chinese Physical Society and IOP Publishing Ltd

step 3D-2D growth process.<sup>[17–19]</sup> The reactor pressure and V/III ratio were maintained at 400 mbar and 2655 for 30 min for 3D growth, and then they were changed to 70 mbar and 199 for 30 min for 2D growth. Then, the reactor temperature was reduced to 700–1000°C to grow the GaN insertion layer, and the growth time was 1–7 min. Finally, the reactor temperature was raised back to 1100°C for another 30 min for 2D growth. Another sample without the GaN insertion layer was grown for comparison. The total thickness of the samples is about 5.5  $\mu\text{m}$ .

The surface morphology of a-plane GaN samples was examined by scanning electron microscopy (SEM) and atomic force microscopy (AFM). The crystal quality of the a-plane GaN samples was characterized us-

ing the x-ray rocking curve-full width at half maximum (XRC-FWHM).

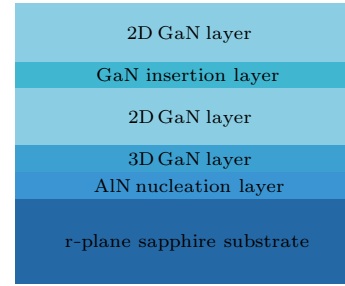


**Fig. 1.** Cross-sectional structural schematic diagram of the nonpolar a-plane GaN samples.

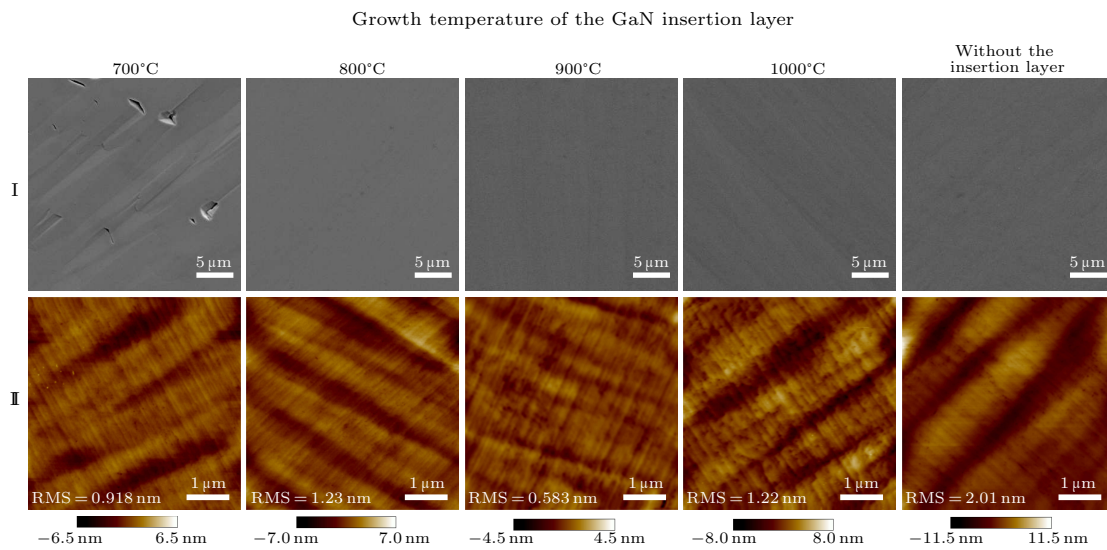


**Fig. 2.** The surface morphology of the nonpolar a-plane GaN samples under different growth temperatures of the GaN insertion layer for (I) plan-view SEM images, and (II) 2-D AFM images (the scanning areas of the AFM images are  $5 \times 5 \mu\text{m}^2$ ). The growth time of the GaN insertion layer was 5 min for all the samples.

Figure 2 shows the SEM and AFM images of samples under different growth temperatures of the GaN insertion layer. The growth time of the GaN insertion layer for all samples was kept for 5 min. As can be seen from the SEM images, triangular pits appeared only in the sample where the insertion layer was grown at 700°C. This means that the low growth temperature of the GaN insertion layer would prevent subsequent growth from forming a flat surface. Further investigation via AFM suggested that the GaN insertion layer significantly ameliorated the roughness of the a-plane GaN samples, especially when growth temperature of the GaN insertion layer was 900°C. The rms roughness of the sample was 0.583 nm, which was 71% less than the sample without the GaN insertion layer. In addition, the streaks on the surface of the sample along the *c*-axis of GaN almost disappeared, which indicates that the introduction of the insertion layer could improve the anisotropy of a-plane GaN surface morphology. These results show that the GaN insertion layer grown at a suitable temperature can moderate

the anisotropy of surface morphology and significantly improve the surface morphology of a-plane GaN.

To further determine the optimal growth condition for the GaN insertion layer, we fixed growth temperature of the GaN insertion layer at 900°C and then changed growth time of the GaN insertion layer. Figure 3 shows the AFM images and the rms roughness of the samples with different growth times of the GaN insertion layer. With the introduction of the GaN insertion layer, the rms roughness of the sample decreases with growth time of the GaN insertion layer. However, when the growth time of the GaN insertion layer is more than 5 min, the roughness of the sample begins to increase significantly. When the growth time of the GaN insertion layer is 3 min, the sample has the smallest rms roughness (0.507 nm). There are no streaks on the surface of the sample along the *c*-axis of GaN. These facts indicate that the growth temperature and the growth time of the GaN insertion layer both affect the surface morphology, and the roughness of the samples is significantly improved by adjusting

these two parameters.

The crystal quality of all the samples was characterized using XRC-FWHM. Figures 4(a) and 4(b) show the XRC-FWHMs of the samples under different growth temperatures of the GaN insertion layer. Suitable growth temperature of the GaN insertion layer can reduce the on-axis XRC-FWHMs, whereas the growth temperature hardly affects the off-axis XRC-FWHMs. We find that the sample has the lowest roughness and the best crystal quality when growth temperature of the GaN insertion layer is 900°C. The FWHMs along *c*-axis and *m*-axis are 546 arcsec and 866 arcsec, respectively; while the FWHMs of the sam-

ple without the GaN insertion layer along *c*-axis and *m*-axis are 676 arcsec and 1040 arcsec. Compared to the sample without the GaN insertion layer, the crystal quality of the samples with the GaN insertion layer is better. However, further changing the growth time of the GaN insertion layer hardly affects the on-axis and off-axis XRC-FWHMs (Figs. 4(c) and 4(d)). In summary, the crystal quality has been improved with the introduction of the GaN insertion layer, and the best crystal quality is obtained when growth temperature of the GaN insertion layer is 900°C and growth time is 5 min.

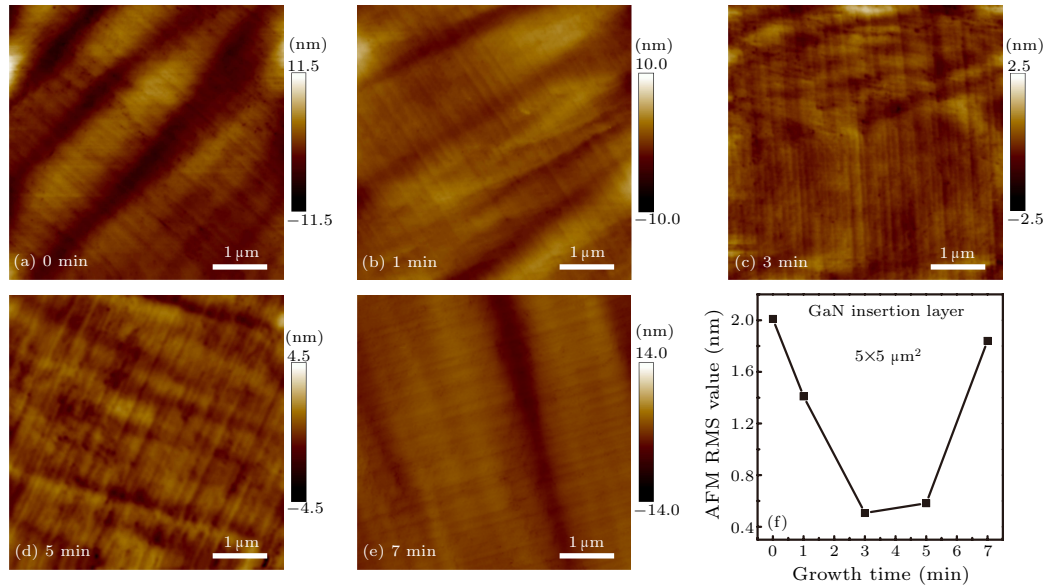


**Fig. 3.** (a)–(e) AFM images of the nonpolar a-plane GaN samples with different growth times of the GaN insertion layer. The scan area is  $5 \times 5 \mu\text{m}^2$ . (f) The rms roughness as a function of growth time of the GaN insertion layer. Growth temperature of the GaN insertion layer was 900°C for all the samples.

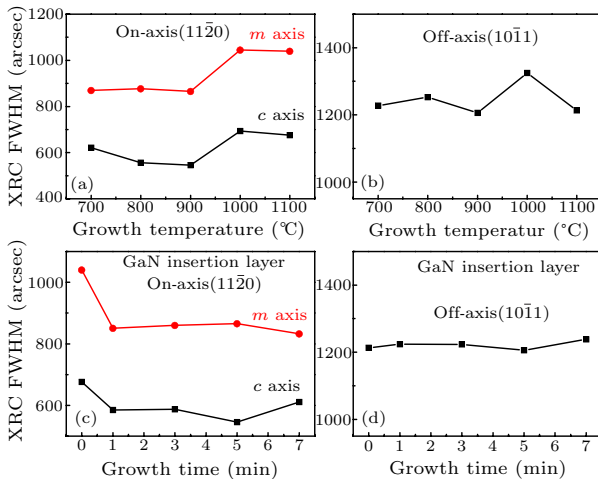


**Fig. 4.** (a) On-axis GaN ( $11\bar{2}0$ ) plane and (b) off-axis GaN ( $10\bar{1}1$ ) plane XRC-FWHMs for the a-plane GaN samples under different growth temperatures of the GaN insertion layer (growth time of the samples was 5 min). (c) On-axis GaN ( $11\bar{2}0$ ) plane and (d) off-axis GaN ( $10\bar{1}1$ ) plane XRC-FWHMs for the a-plane GaN samples with different growth times of the GaN insertion layer (growth temperature of the samples was 900°C).

To explore the mechanisms for the improvement of surface morphology with the introduction of the GaN insertion layer, we prepared two samples by terminating the epitaxy after or before growth of the GaN insertion layer. The growth temperature of the GaN insertion layer was 900°C, and the growth time was 3 min. As can be seen from Figs. 5(a) and 5(c), many small holes appear on the surface of the sample terminated after growth of the GaN insertion layer, while there is no hole on the surface of the sample terminated before growth of the GaN insertion layer (Figs. 5(b) and 5(d)). Streaks along *c*-direction can be observed in both the samples, and the surface fluctuation of the sample with the GaN insertion layer becomes larger. Figures 5(e) and 5(f) are the 3-D AFM images of the samples with and without the GaN insertion layer. Streaks along *c*-direction can hardly be observed on the surface of the sample with the GaN insertion layer, and the holes also disappear after 30 min of 2D growth (Fig. 5(e)). However, streaks along *c*-direction can still be seen in Fig. 5(f). There is no obvious difference between the sample grown after 30 min

of 2D growth with the sample grown after 60 min of 2D growth. The surface morphology of the sample in Figs. 5(a) and 5(c) is similar to the surface morphology during the 3D-2D growth transition reported in the literature.<sup>[19]</sup> In our experiment, the rough mor-

phology induced by the GaN insertion layer probably triggers the secondary 3D-2D growth process, thereby eliminating the streaks along the *c*-direction, reducing the surface roughness and improving the surface morphology.

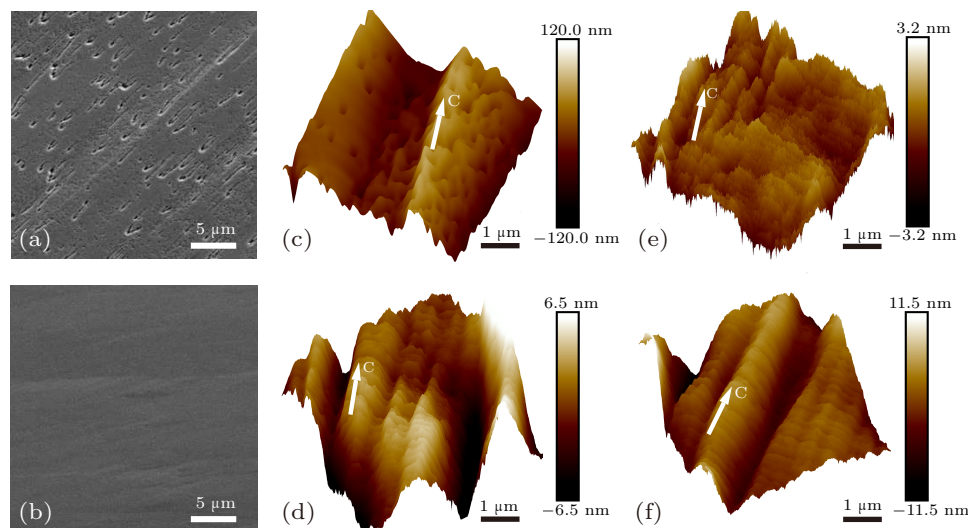


**Fig. 5.** The SEM and AFM images of the samples prepared by terminating the epitaxy after [(a), (c)] and before [(b), (d)] growth of the GaN insertion layer, and the 3-D AFM images of a-plane GaN samples (e) with the GaN insertion layer (growth temperature was 900°C, and growth time was 3 min) and (f) without the GaN insertion layer.

In conclusion, we have systematically studied the effects of the growth conditions of the low-temperature GaN insertion layers on the surface morphology of non-polar a-plane GaN. When the growth temperature of the GaN insertion layer is 900°C and the growth time is 3 min, we obtain an rms roughness as small as 0.507 nm. The improvement of surface morphology could come from the reason that the GaN insertion layer leads to the secondary 3D-2D growth process. These results indicate that the low-temperature GaN insertion layer is a simple and effective method for improving the surface morphology of non-polar a-plane GaN.

## References

- [1] Moustakas T D and Paiella R 2017 *Rep. Prog. Phys.* **80** 106501
- [2] Zeng F, An J X, Zhou G, Li W, Wang H, Duan T, Jiang L and Yu H 2018 *Electronics* **7** 377
- [3] Schmidt M C, Kim K C, Sato H, Fellows N, Masui H, Nakamura S, DenBaars S P and Speck J S 2007 *Jpn. J. Appl. Phys.* **46** L126
- [4] Wetzel C, Zhu M, Senawiratne J, Detchprohm T, Persans P D, Liu L, Preble E A and Hanser D 2008 *J. Cryst. Growth* **310** 3987
- [5] Masui H, Nakamura S, DenBaars S P and Mishra U K 2010 *IEEE Trans. Electron Devices* **57** 88
- [6] Craven M D, Lim S H, Wu F, Speck J S and DenBaars S P 2002 *Appl. Phys. Lett.* **81** 469
- [7] Bai J, Jiu L, Gong Y and Wang T 2018 *Semicond. Sci. Technol.* **33** 125023
- [8] Jiu L, Gong Y and Wang T 2018 *Sci. Rep.* **8** 9898
- [9] Wang H M, Chen C Q, Gong Z, Zhang J P, Gaevski M, Su M, Yang J W and Khan M A 2004 *Appl. Phys. Lett.* **84** 499
- [10] Lee Y S, Kim H, Seo T H, Park A H, Lee S B, Chung S J, Choi C J and Suh E K 2013 *Electron. Mater. Lett.* **9** 587
- [11] Son J S, Honda Y, Yamaguchi M, Amano H, Baik K H, Seo Y G and Hwang S M 2013 *Thin Solid Films* **546** 108
- [12] Die J H, Wang C W, Yan S, Hu X T, Hu W, Ma Z G, Deng Z, Du C H, Wang L, Jia H Q, Wang W X, Jiang Y and Chen H 2019 *Appl. Phys. Express* **12** 015503
- [13] Wang C W, Jiang Y, Die J H, Yan S, Hu X T, Hu W, Ma Z G, Deng Z, Jia H Q and Chen H 2019 *CrystEngComm* **21** 2747
- [14] Chakraborty A, Kim K C, Wu F, Speck J S, DenBaars S P and Mishra U K 2006 *Appl. Phys. Lett.* **89** 041903
- [15] Xu S R, Zhang J C, Yang L A, Zhou X W, Cao Y R, Zhang J F, Xue J S, Liu Z Y, Ma J C, Bao F and Hao Y 2011 *J. Cryst. Growth* **327** 94
- [16] Chen C Q, Yang J W, Wang H M, Zhang J P, Adivarahan V, Gaevski M, Kuokstis E, Gong Z, Su M and Khan M A 2003 *Jpn. J. Appl. Phys.* **42** L640
- [17] Araki M, Mochimizo N, Hoshino K and Tadatomo K 2007 *Jpn. J. Appl. Phys.* **46** 555
- [18] Johnston C F, Kappers M J and Humphreys C J 2009 *J. Appl. Phys.* **105** 073102
- [19] Sun Q, Kong B H, Yerino C D, Ko T S, Leung B, Cho H K and Han J 2009 *J. Appl. Phys.* **106** 123519